Soot Formation Modelling of n-Heptane Spray Combustion Under Diesel Engine Conditions Using the Conditional Moment Closure Approach

Michele Bolla, Yuri M. Wright and Kostantinos Boulouchos
Aerothermochemistry and Combustion Systems Laboratory, ETH Zurich, Switzerland
E-mail: mbolla@lav.mavt.ethz.ch

Methodology

In this poster first results of numerical simulations of soot formation of n-heptane spray in a constant-volume vessel under Diesel engine conditions different ambient oxygen molar concentrations (8-21% O_2 range) are presented. Results were validated against high-fidelity measurements from the Sandia constant-volume combustion chamber facility [1, 2], which consists of a cubic shape with 108 mm side length. The experimental temperature and pressure were in all cases 1000 K and approximately 42 bar, respectively.

The numerical flow field was solved with the commercial computational fluid dynamics (CFD) solver STAR-CD [3] coupled with an elliptic first order conditional moment closure based combustion model [4, 5] with standard closure modeling approaches for conditional velocity, conditional scalar dissipation rate and conditional turbulent fluxes as proposed in [5]. The high Reynolds number k-ε-RNG turbulence model [3] is used. Fuel spray droplets are treated in an Eulerian-Lagrangian way with STAR-CD built-in primary and secondary breakup models [6, 7]. The reduced n-Heptane chemical mechanism by Liu et al. [8] consisting of 22 species and 18 global reactions is used.

Soot formation is modeled with the semi-empirical two-equations model of Leung [9], where simultaneous soot particle inception, surface growth, coagulation and oxidation by O_2 and OH are considered. In the current implementation, particle inception rate is a first order function of acetylene concentration only. Transport equations for soot mass fraction and soot number density were solved with unity Lewis number assumption, neglecting differential diffusion effects of soot particles, whose size distribution was assumed as mono-dispersed. Radiation of soot particles was modeled with an optical-thin formulation after [10] using soot mean absorptivity values from [11].

Results

Ignition delay time was overpredicted for all ambient oxygen concentrations considered. Discrepancy became larger with lower oxygen presence. However, increasing ignition delay times by diminishing oxidizer content was well captured. The same trend for lift-off heights was observed, i.e. increased lift-off heights by reducing ambient oxidizer amount. Simulation trend was fairly predicted. The influence of the ambient oxygen mole fraction on the flame structure is analyzed on the basis of the 21% and 10% O_2 cases. Flame characteristics relevant for soot behavior (mixture fraction, temperature, mass fractions of OH, O_2 and C_2H_2) are illustrated for the two different cases at 5 ms during the quasi steady-state period. The main difference consists in the lower stochiometric mixture fraction for the 10% O_2 case. As a consequence the stochiometric region becomes larger and therefore the entire flame becomes broader. Maximal stochiometric axial distances were approximately 75 mm and 105 mm for 21% and 10% O_2, respectively. With a lower ambient O_2 concentration, as expected, a lower flame temperature

was observed due to the reduced oxidizer availability. All chemical processes are shifted farther downstream from the injector. Mass fractions of C_2H_2 and OH are roughly one order of magnitude lower compared to the 21% O_2 case.

Soot volume fraction during quasi-steady spray behavior between 3-6 ms was compared with experiment [1] which was performed with laser induced incandescence methodology. Experimental soot distribution was measured until approximately 90 mm axial distance from the injector tip. Soot was observed in the fuel rich zone. In the 21% O_2 case, the entire soot-loaded region was visualized in the experiment, instead for the 10% case peak soot concentration is expected to be out of sight.

Soot volume fraction distribution with the higher oxygen content was well predicted. For the lower oxidizer concentration peak soot volume fraction was overpredicted, although experimental maximal soot concentration was not in the observation region. A lower soot amount and a farther downstream location from the injector with lower oxygen concentration were both predicted correctly. Soot mass fraction an number density distribution and the accordingly source terms are presented in mixture fraction space at the location of peak soot volume fraction.

Soot mass fraction is present only in the fuel rich region and reaches the peak at an equivalence ration of around two for both ambient oxygen concentrations considered. In contrast to the mass fraction, the number density does appear in the fuel lean region because soot particle oxidation is assumed to reduce particle mass but not the particle number. However presence of particles with negligible mass in the fuel lean region do not influence soot volume fraction in space. The relative contribution of oxidation by OH plays an important role only for the 21% O_2 case due to the higher OH/O_2 concentration ratio present in the flame. Molecular diffusion of soot mass fraction towards stochiometry is mainly balanced with oxidation by OH and O_2.

First results suggest that the conditional moment closure combustion model approach can be considered a promising framework for soot modeling because of the accurate flame structure description, which is essential for soot predictions.

References

[1]   C. A. Idicheria and L. M. Pickett, "Soot Formation in Diesel Combustion under High-EGR Conditions," *SAE2005-01-3834,* 2005.

[2]   L. M. Pickett, "Engine Combustion Network," *sandia.gov/enc/sprayCombustion.php,* 2011.

[3]   CD-adapco, "Methodology StarCD Version 4.14," 2010.

[4]   Y. M. Wright*, et al.*, "Simulations of spray autoignition and flame establishment with two-dimensional CMC," *Combustion and Flame,* vol. 143, pp. 402-419, Dec 2005.

[5]   A. Y. Klimenko and R. W. Bilger, "Conditional moment closure for turbulent combustion," *Progress in Energy and Combustion Science,* vol. 25, pp. 595-687, 1999.

[6]   K. Y. Huh and A. D. Gosman, "A phenomenological model of Diesel spray atomization," presented at the Proc. Int. Conf. on Multiphase Flows (ICMF '91), Tsukuba, 1991.

[7]   R. D. Reitz and R. Diwakar, "Structure of high-pressure fuel spray," *SAE870598,* 1987.

[8]   S. L. Liu*, et al.*, "Effects of strain rate on high-pressure nonpremixed n-heptane autoignition in counterflow," *Combustion and Flame,* vol. 137, pp. 320-339, May 2004.

[9]   K. M. Leung*, et al.*, "A Simplified Reaction-Mechanism for Soot Formation in Nonpremixed Flames," *Combustion and Flame,* vol. 87, pp. 289-305, Dec 1991.

[10]   B. Marracino and D. Lentini, "Radiation modelling in non-luminous nonpremixed turbulent flames," *Combustion Science and Technology,* vol. 128, pp. 23-48, 1997.

[11]   J. F. Widmann, "Evaluation of the planck mean absorption coefficients for radiation transport through smoke," *Combustion Science and Technology,* vol. 175, pp. 2299-2308, Dec 2003.

M. Bolla   mbolla@lav.mavt.ethz.ch
Y. M. Wright   wright@lav.mavt.ethz.ch
Prof. K. Boulouchos boulouchos@lav.mavt.ethz.ch

SOOT MODELLING

Soot Formation Modelling of n-Heptane Spray Combustion Under Diesel Engine Conditions Using the Conditional Moment Closure Approach

INTRODUCTION

Diesel engines offer a very high efficiency and are therefore widely used in power generation and transportation. Soot emissions by Diesel engines are dangerous for the enviroment and for living organisms. Governement legislations for soot emissions are becoming even more stringent, therefore there is the need to better understand the physics of soot formation at those conditions.

In this numerical study, the influence of ambient oxygen concentration on spray flame characteristics and soot formation is investigated. Prediction of preprocesses, e. g. two-phase flow and flame dynamics are a prerequisite for soot modeling.

EXPERIMENTAL SETUP [1,2]

Sandia constant-volume combustion vessel [1]
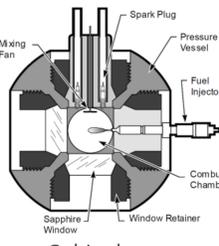
Ambient temperature	1000 K
Ambient density	14.8 kg/m³
Ambient pressure	~ 42 bar
O2 molar fraction	8-10-12-15-21 %
Fuel type	n-Hepane
Injection pressure	1500 bar
Injection duration	~ 7 ms
Tot. inj. fuel mass	~ 18 mg
Nozzle diameter	0.100 mm
Nozzle L/D	4

Cubic shape
(108 mm side)

Table 1: Experimental configuration

Measurement techniques: OH* chem. (flame lift-off)
                         LII (soot volume fraction)

CFD MODEL

CFD computational setup:

- Commercial CFD code STAR-CD [3]
- 2D grid with 0.5 mm mesh size
- RANS, k-ε turbulence model, wall functions
- Euler-Langrange approach for droplets
- Coditional Moment Closure (CMC) combustion model [4]
- Reduced mechanism for n-heptane [6]
- Two-equations soot model [7]
- Optical-thin soot radiation model [8,9]
- Soot differential diffusion effects neglected (Le=1)

SOOT MODEL: TWO-EQUATIONS MODEL [7]
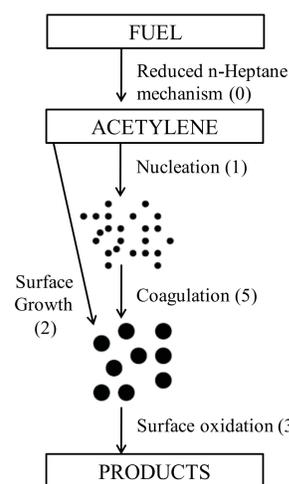
(1) Particle inception:
$$C_2H_2 \rightarrow 2C_{(S)} + H_2$$
$$\dot{\omega}_{INCP} = 10^4 [C_2H_2] e^{-\frac{21100}{T}}$$

(2) Particle surface growth
$$C_2H_2 + nC_{(S)} \rightarrow (n+2)C_{(S)} + H_2$$
$$\dot{\omega}_{SUR\,GROW} = 6 \cdot 10^3 [C_2H_2] e^{-\frac{12100}{T}} \cdot \sqrt{A_{soot}}$$

(3) Particle oxidation by O_2:
$$C_{(S)} + \frac{1}{2}O_2 \rightarrow CO$$
$$\dot{\omega}_{OXID_{O_2}} = 10^4 [O_2] e^{-\frac{19000}{T}} \cdot \sqrt{T} \cdot A_{soot}$$

(4) Particle oxidation by OH:
$$C_{(S)} + OH \rightarrow CO + H$$
$$\dot{\omega}_{OXID_{OH}} = 0.36 [OH] \cdot \sqrt{T} \cdot A_{soot}$$

(5) Particle coagulation:
$$nP \rightarrow P_n$$
$$\dot{\omega}_{COAG} = -3 \left(\frac{24R}{\rho_S N_A} \right)^{\frac{1}{2}} \left(\frac{6}{\pi \rho_S} \right)^{\frac{1}{6}} T^{\frac{1}{2}} (\rho Y_S)^{\frac{1}{6}} N_S^{\frac{11}{6}}$$

Soot model accouts for simultaneous soot particle inception, surface growth, oxidation by O_2 and OH and coagulation

Solve transport equations for soot mass fraction and soot number density (Le=1):

$$\frac{\partial Q_\alpha}{\partial t} + \langle u_i | \eta \rangle \frac{\partial Q_\alpha}{\partial x_i} - \langle N | \eta \rangle \frac{\partial^2 Q_\alpha}{\partial \eta^2} + \frac{1}{\bar{\rho}\tilde{P}(\eta)} \frac{\partial}{\partial x_i} \left[\langle \rho u_i'' Y_\alpha'' | \eta \rangle \tilde{P}(\eta) \right] = \langle w_\alpha | \eta \rangle$$

Source term soot mass fraction:

$$\langle w_{Y_S} | \eta \rangle = \langle w_{Y_S,inception} | \eta \rangle + \langle w_{Y_S,growth} | \eta \rangle + \langle w_{Y_S,oxidationO_2} | \eta \rangle + \langle w_{Y_S,oxidationOH} | \eta \rangle$$

Source term soot number density:

$$\langle w_{N_S} | \eta \rangle = \langle w_{N_S,inception} | \eta \rangle + \langle w_{N_S,coagulation} | \eta \rangle$$

GOVERNING EQUATIONS [4]

$$\frac{\partial Q_\alpha}{\partial t} + \langle u_j | \eta \rangle \frac{\partial Q_\alpha}{\partial x_j} = \langle N | \eta \rangle \frac{\partial^2 Q_\alpha}{\partial \eta^2} + \langle w_\alpha | \eta \rangle - \frac{1}{\bar{\rho}\tilde{P}(\eta)} \frac{\partial}{\partial x_j} \left[\langle u_j'' y_\alpha'' | \eta \rangle \bar{\rho} \tilde{P}(\eta) \right]$$

$$\langle u_i'' y_\alpha'' | \eta \rangle = -D_t \frac{\partial Q_\alpha}{\partial x_j}$$ Gradient flux

$$\langle u_i | \eta \rangle = \tilde{u}_i - \frac{D_t}{\tilde{\varsigma''^2}} \frac{\partial \tilde{\varsigma}}{\partial x_j} (\eta - \tilde{\varsigma})$$ Linear model for conditional velocity
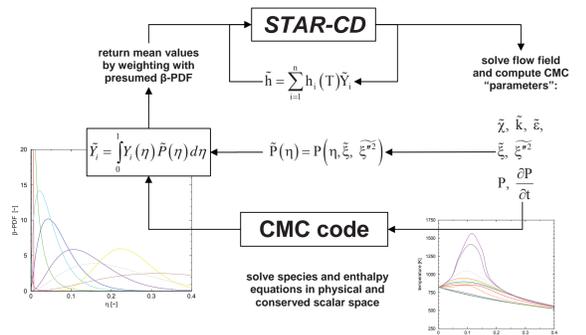
$$\langle w_\alpha | \eta \rangle = \dot{\omega}_\alpha (Q_\alpha, Q_T, P)$$ First order closure for the source terms

$$\langle N | \eta \rangle = \frac{\tilde{\chi}}{2 \int_0^1 G(\eta) \tilde{P}(\eta) d\eta} \frac{\exp \left(-2 \left[erf^{-1}(2\eta - 1) \right]^2 \right)}{G(\eta)}$$ AMC model for the scalar dissipation rate

$$\langle w_{RAD} | \eta \rangle = -4\sigma \alpha_{soot} \left[\langle T | \eta \rangle^4 - T^4_{Wall} \right]$$ Optical-thin assumption for soot radiation [8,9]
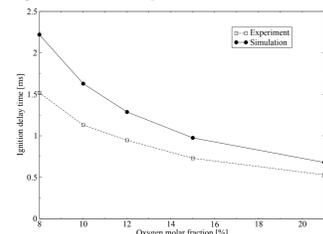$$\alpha_{soot} = 2370 \frac{1}{mK} \cdot f_{v,soot} \cdot T$$
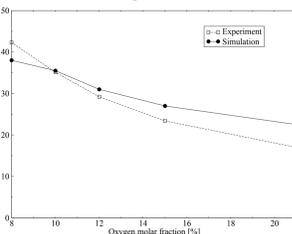
Interfacing of CFD and CMC code [5]:

## RESULTS: FLAME STRUCTURE

Ignition delay time validation

Lift-off height validation

Influence of ambient O_2 concentration:

with *lower O_2*:

- Higher ignition delay time
- Higher lift-off height
- Lower stochiometric mixture fraction
- Broader flame
- Lower flame temperature
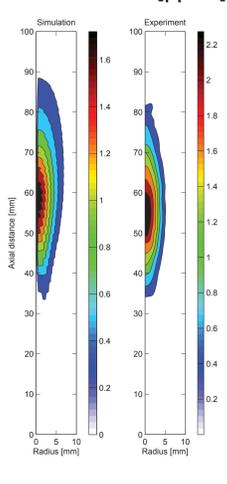- Lower C_2H_2, O_2, OH concentrations

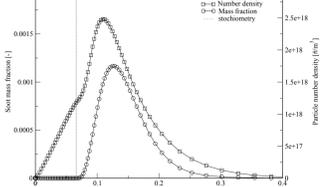### Flame characteristics relevant for soot behavior at 5 ms (quasi steady-state)

21 % O_2 ($\xi_{st.}$=0.061)

10 % O_2 ($\xi_{st.}$=0.03)
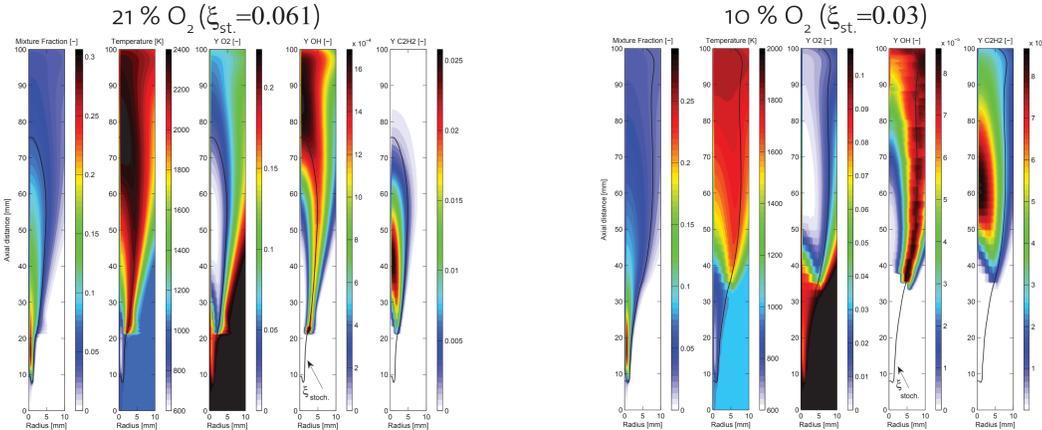
RESULTS: SOOT FORMATION

21 % O_2 ($\xi_{st.}$=0.061)

volume fraction [ppmv]
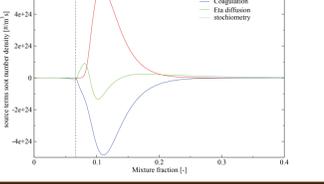
10 % O_2 ($\xi_{st.}$=0.03)

volume fraction [ppmv]
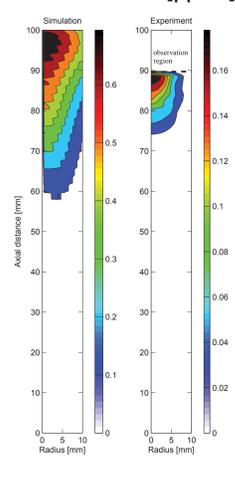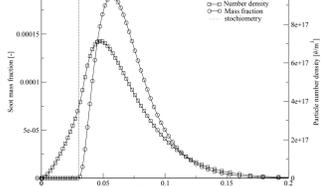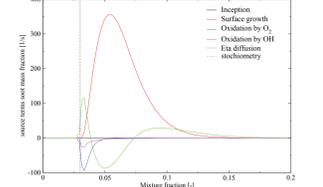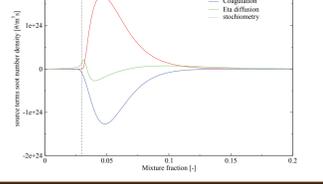
REFERENCES

[1] L. M. Pickett, „Engine Combustion Network, www. sandia.gov/enc/sprayCombustion.php, 2011.

[2] C. A. Idicheria and L. M. Pickett, „Soot Formation in Diesel Combustion under High-EGR Conditions," SAE2005-01-3834, 2005.

[3] CD-adapco, STAR-CD v4.14, 2010.

[4] A. Y. Klimenko and R. W. Bilger, „Conditional moment closure for turbulent combustion," Progress in Energy and Combustion Science, vol. 25, pp. 595-687, 1999.

[5] Y. M. Wright, et al., „Simulations of spray autoignition and flame establishment with two-dimensional CMC," Combustion and Flame, vol. 143, pp. 402-419, 2005.

[6] S. L. Liu, et al., „Effects of strain rate on high-pressure nonpremixed n-heptane autoignition in counterflow," Combustion and Flame, vol. 137, pp. 320-339, 2004.

[7] K. M. Leung, et al., „A Simplified Reaction-Mechanism for Soot Formation in Nonpremixed Flames," Combustion and Flame, vol. 87, pp. 289-305, 1991.

[8] B. Marracino and D. Lentini, „Radiation modelling in non-luminous nonpremixed turbulent flames," Combustion Science and Technology, vol. 128, pp. 23-48, 1997.

[9] J. F. Widmann, „Evaluation of the planck mean absorption coefficients for radiation transport through smoke," Combustion Science and Technology, vol. 175, pp.

ACKNOWLEDGEMENTS

Laboratorium für Aerothermochemie und Verbrennungssysteme
Aerothermochemistry and Combustion Systems Laboratory

Eidgenössische Technische Hochschule Zürich
Swiss Federal Institute of Technology Zurich

ETH